


**Aharonov-Bohm effect in mesoscopic Bose-Einstein condensates**Tobias Haug <sup>1</sup>, Hermanni Heimonen,<sup>1</sup> Rainer Dumke,<sup>1,2,3</sup> Leong-Chuan Kwek,<sup>1,3,4,5</sup> and Luigi Amico<sup>1,3,6,7,8</sup><sup>1</sup>*Centre for Quantum Technologies, National University of Singapore, 3 Science Drive 2, Singapore 117543, Singapore*<sup>2</sup>*Division of Physics and Applied Physics, Nanyang Technological University, 21 Nanyang Link, Singapore 637371, Singapore*<sup>3</sup>*MajuLab, CNRS-UNS-NUS-NTU International Joint Research Unit, UMI 3654, Singapore*<sup>4</sup>*Institute of Advanced Studies, Nanyang Technological University, 60 Nanyang View, Singapore 639673, Singapore*<sup>5</sup>*National Institute of Education, Nanyang Technological University, 1 Nanyang Walk, Singapore 637616, Singapore*<sup>6</sup>*Dipartimento di Fisica e Astronomia, Via S. Sofia 64, I-95127 Catania, Italy*<sup>7</sup>*CNR-MATIS-IMM & INFN-Sezione di Catania, Via S. Sofia 64, I-95127 Catania, Italy*<sup>8</sup>*LANEF “Chaire d’excellence,” Université Grenoble-Alpes & CNRS, F-38000 Grenoble, France*

(Received 9 August 2017; revised manuscript received 18 January 2018; published 4 October 2019)

Ultracold atoms in light-shaped potentials open up new ways to explore mesoscopic physics: Arbitrary trapping potentials can be engineered with only a change of the laser field. Here, we propose using ultracold atoms in light-shaped potentials to feasibly realize a cold-atom device to study one of the fundamental problems of mesoscopic physics, the Aharonov-Bohm effect: the interaction of particles with a magnetic field when traveling in a closed loop. Surprisingly, we find that the Aharonov-Bohm effect is washed out for interacting bosons, while it is present for fermions. We show that our atomic device has possible applications as a quantum simulator, Mach-Zehnder interferometer, and for tests of quantum foundation.

DOI: [10.1103/PhysRevA.100.041601](https://doi.org/10.1103/PhysRevA.100.041601)**I. INTRODUCTION**

The Aharonov-Bohm effect is one of the most striking manifestations of quantum mechanics: Due to phase shifts in the wave function, specific interference effects arise when charged particles enclose a region with a nonvanishing magnetic field [1]. This effect has important implications in the foundational aspects of quantum physics [1–4] and many-body quantum physics [5–9]. The Aharonov-Bohm effect has been influential in many fields of physical sciences, such as mesoscopic physics, quantum electronics, and molecular electronics [10–13], with remarkable applications enabling quantum technologies [14–19].

An electronic fluid confined to a ring-shaped wire pierced by a magnetic flux is the typical configuration employed to study the Aharonov-Bohm effect. In this way, a matter-wave interferometer is realized: The current through the ring-shaped quantum system displays characteristic oscillations depending on the imparted magnetic flux. Neutral particles with magnetic moments display similar interference effects [20].

A different perspective to study the transport through small- and medium-sized quantum matter systems has been demonstrated recently in ultracold atoms [21–24]: In such systems, it is possible to manipulate and adjust the carrier statistics, particle-particle interactions, and spatial configuration of the circuit. Such flexibility is very hard, if not impossible, to achieve using standard realizations of mesoscopic systems. Mesoscopic phenomena are studied predominantly with electrons in condensed-matter devices. The range of parameters that can be explored is limited since a single change in a parameter requires a new device or may not be

possible at all. To adjust all those parameters, atomtronics has been put forward [25–27].

In this Rapid Communication, we study the Aharonov-Bohm effect in a mesoscopic ring-shaped bosonic condensate pierced by a synthetic magnetic flux [28]: The bosonic fluid is injected from a “source” lead, propagates along the ring, and it is collected in a “drain” lead. In this way, we provide the atomtronic counterpart of an iconic problem in mesoscopic physics [10,11], with far reaching implications over the years in the broad area of physical science [5–9,14–19]. This system can realize an elementary component of an atomtronic integrated circuit [29]. We analyze the nonequilibrium dynamics of the system by quenching the particles’ spatial confinement; our study is combined with an analysis of the out-of-equilibrium dynamics triggered by driving the current through suitable baths attached to the system within Markovian approximations and an exact simulation using density matrix renormalization group (DMRG). Depending on the ring-lead coupling, interactions, and particle statistics, the system displays qualitatively distinct nonequilibrium regimes characterized by the different response of the interference pattern to the effective gauge field. Remarkably, the interacting bosonic system lacks the fundamental Aharonov-Bohm effect as it is washed out, in contrast to a fermionic system. Finally, we explore possible applications of this device to realize atomtronic quantum devices, quantum simulators, and tests for the quantum foundation.

**II. MODEL**

The Bose-Hubbard Hamiltonian  $\mathcal{H} = \mathcal{H}_r + \mathcal{H}_l$  describes the system consisting of a ring with an even number of lattice

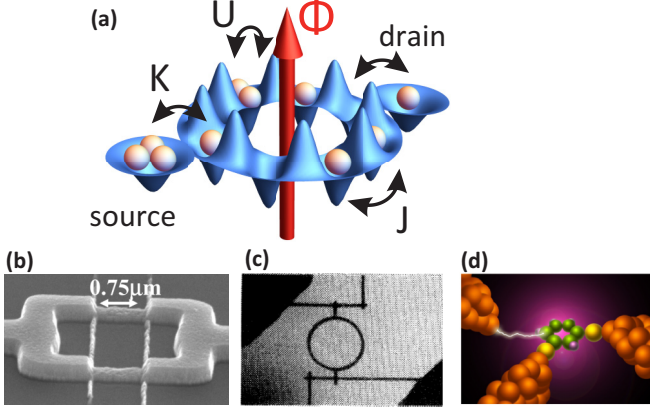


FIG. 1. Mesoscopic systems and its analogous atomtronic architecture. (a) Atomtronic setup consisting of a superfluid condensate in a ring lattice with two attached leads. The dynamics is controlled by Aharonov-Bohm flux  $\Phi$  and ring-lead coupling  $K$ . Atoms tunnel between ring sites with rate  $J$  and interact on site with strength  $U$ . Related mesoscopic condensed-matter devices to study the Aharonov-Bohm effect are (b) superconducting interference devices [30], (c) nanoscopic metal rings [12], and (d) the proposed molecular quantum device [19].

sites  $L$  and two leads (see Fig. 1). The ring Hamiltonian is given by

$$\mathcal{H}_r = - \sum_{j=0}^{L-1} (J e^{i2\pi\Phi/L} \hat{a}_j^\dagger \hat{a}_{j+1} + \text{H.c.}) + \frac{U}{2} \sum_{j=0}^{L-1} \hat{n}_j (\hat{n}_j - 1), \quad (1)$$

where  $\hat{a}_j$  and  $\hat{a}_j^\dagger$  are the annihilation and creation operators at site  $j$ ,  $\hat{n}_j = \hat{a}_j^\dagger \hat{a}_j$  is the particle number operator,  $J$  is the intraring hopping,  $U$  is the on-site interaction between particles, and  $\Phi$  is the total flux through the ring. Periodic boundary conditions are applied:  $\hat{a}_L^\dagger = \hat{a}_0^\dagger$ .

The two leads dubbed the source (S) and drain (D) consist of a single site each, which are coupled symmetrically at opposite sites to the ring with coupling strength  $K$ . In both of them, the local potential energy and on-site interaction are set to zero as the leads are considered to be large with a low atom density. The lead Hamiltonian is  $\mathcal{H}_l = -K(\hat{a}_S^\dagger \hat{a}_0 + \hat{a}_D^\dagger \hat{a}_{L/2} + \text{H.c.})$ , where  $\hat{a}_S^\dagger$  and  $\hat{a}_D^\dagger$  are the creation operators of source and drain, respectively.

The system is initially prepared with all particles in the source and the dynamics is strongly affected by the lead-ring coupling. We calculate the state at time  $t$  with  $|\Psi(t)\rangle = e^{-i\mathcal{H}t} |\Psi(0)\rangle$ . We investigate the expectation value of the density in the source and drain over time, which for the source is calculated as  $n_{\text{source}}(t) = \langle \Psi(t) | \hat{a}_S^\dagger \hat{a}_S | \Psi(t) \rangle$  and similar for the drain. We point out that, by construction, our approach is well defined for the whole crossover ranging from the weak to strong lead-system coupling (in contrast with the limitations of traditional approaches for interacting particles mostly valid for the regime of weak lead-system coupling [31]). We assume that the motion of the atoms involves only the lowest Bloch band, thus providing a purely one-dimensional dynamics. Our results are given in units of the tunneling rate  $J$  between neighboring ring sites. It

depends exponentially on the lattice spacing. In state-of-the-art experiments on cold atoms in lattices,  $J/\hbar \approx 250\text{--}500$  Hz was reported [32,33] and atom lifetimes of 8 s [34]. In experiments, this would restrict the maximal observation time  $t$  in units of  $J$  to  $tJ = 2000\text{--}4000$ .

### III. RESULTS

In the weak-coupling regime  $K/J \ll 1$ , the lead-ring tunneling is slow compared to the dynamics inside the ring. In this regime, the condensate mostly populates the drain and source, leaving the ring nearly empty. As a result, the scattering due to the on-site interaction  $U$  has a negligible influence on the dynamics. With increasing  $\Phi$  the oscillation becomes faster and the ring populates, resulting in increased scattering and washed-out density oscillations.

In the strong-coupling regime  $K/J \approx 1$ , the lead-ring and the intraring dynamics are characterized by the same frequency and cannot be treated separately. Here, a superposition of many oscillation frequencies appears (see also Supplemental Material [35]), and after a short time the condensate is evenly spread both in leads and ring [Figs. 2(d)–2(f)]. The density in the ring is large and scattering affects the dynamics by washing out the oscillations. Close to  $\Phi = 0.5$ , the oscillations slow down, especially for a weak interaction,

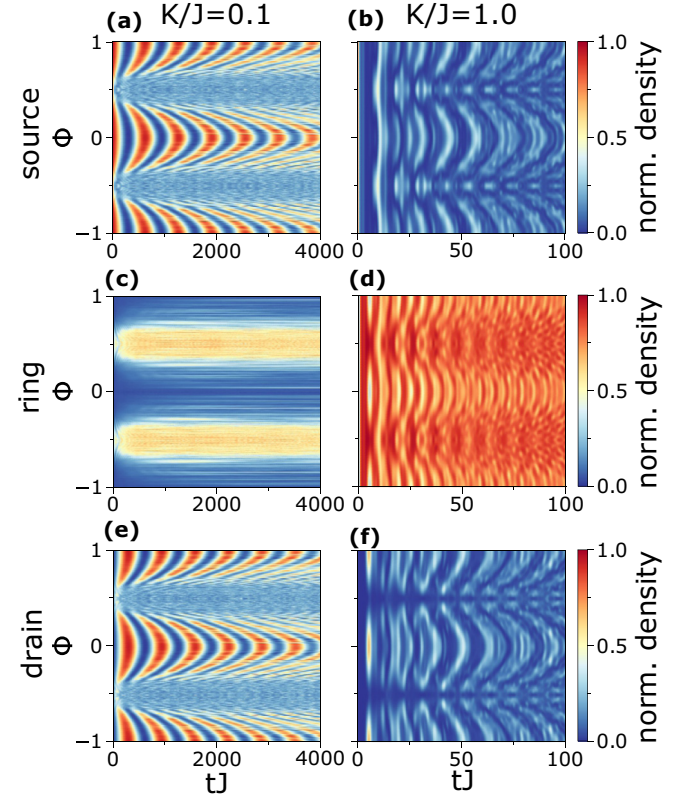


FIG. 2. Time evolution of density in (a), (b) source, (c), (d) ring, and (e), (f) drain plotted against flux  $\Phi$ . (a), (c), (e) Weak ring-lead coupling  $K/J = 0.1$  (on-site interaction  $U/J = 5$ ). (b), (d), (f) Strong ring-lead coupling  $K/J = 1$  ( $U/J = 0.2$ ). Time is indicated  $tJ$  in units of inter-ring tunneling parameter  $J$ . The number of ring sites is  $L = 14$  with  $N_p = 4$  particles initially in the source. The density in the ring is  $n_{\text{ring}} = 1 - n_{\text{source}} - n_{\text{drain}}$ .

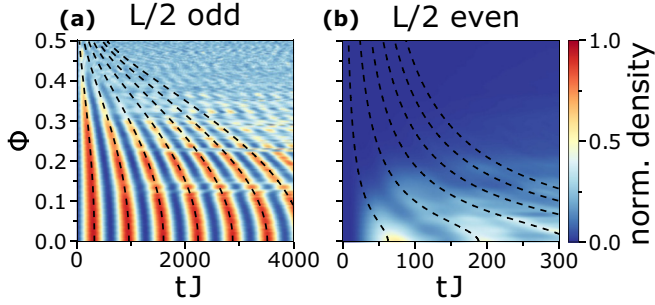


FIG. 3. Density in the drain against flux  $\Phi$  and parity in the number of ring sites with (a) odd parity  $L/2 = 7$  ( $U/J = 3$ ) and (b) even parity  $L/2 = 8$  ( $U/J = 1$ ). Simulation with  $N_p = 4$  and weak coupling ( $K/J = 0.1$ ). The structures around  $\Phi = 0.15$  for odd parity are many-body resonances [37]. The dashed line shows the analytic derived oscillation period [(a) Eq. (10) and (b) Eq. (3) in the Supplemental Material [35]].

due to destructive interference [36]. We studied the dynamics of the relative phase between the source and drain: We find that relative phase displays similar dynamics as the source and drain density (see Supplemental Material [35]).

We also find that the dynamics is affected by the parity in half of the number of ring sites  $L/2$ , especially in the weak-coupling regime. In Fig. 3, we find that for odd ( $L/2 = 3, 5, 7, \dots$ ) and even parity ( $L/2 = 2, 4, 6, \dots$ ) the flux dependence and timescales differ widely. Similar to tunneling through quantum dots, we can understand the parity effect in terms of ring-lead resonant and off-resonant coupling [38]. Off-resonant coupling is characterized by regular, slow oscillations between the source and drain and a small ring population. Resonant coupling implies faster oscillation, but a large ring population. The resulting dynamics is affected by the interplay between interaction  $U$  and  $\Phi$ . The flux  $\Phi$  modifies the energy eigenmodes of the ring, bringing them in and out of resonance with the leads. Interaction  $U$  washes out the oscillations between the source and drain when the ring population is large. For odd parity, we find that both resonant and off-resonant coupling contributes. Close to  $\Phi = 0$ , the off-resonant coupling dominates and due to the small ring population the interaction has only a minor effect on the dynamics. Close to  $\Phi = 0.5$ , resonant ring modes become dominant, and the faster oscillations are washed out by the higher ring population. For even parity only resonant coupling is possible. Close to  $\Phi = 0$ , ring modes are on resonance, resulting in fast oscillations washed out by the interaction. For increasing  $\Phi$  transfer is suppressed as the ring modes move out of resonance and off-resonant coupling is not possible (see the detailed derivation in the Supplemental Material [35]). Parity effects are suppressed with strong coupling or many ring sites as the level spacing decreases and many ring modes can become resonant.

*Open system.* To study the properties of a filled ring, in Fig. 4 we couple particle reservoirs with the leads to drive a current through the now open system. We model it using the Lindblad master equation

$$\frac{\partial \rho}{\partial t} = -\frac{i}{\hbar} [H, \rho] - \frac{1}{2} \sum_m \{ \hat{L}_m^\dagger \hat{L}_m, \rho \} + \sum_m \hat{L}_m \rho \hat{L}_m^\dagger$$

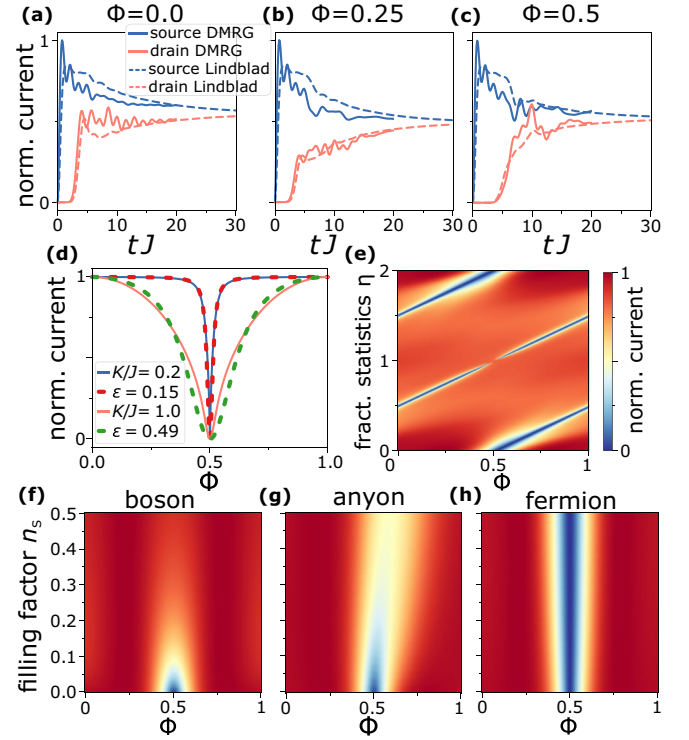


FIG. 4. Current through the Aharonov-Bohm ring. (a)–(c) Evolution of source and drain current towards the steady state (when both currents are the same) with DMRG (solid line) and Lindblad formalism (dashed) for hard-core bosons,  $K = 1$  and  $L_R = 10$ . For DMRG, both reservoirs and the ring are solved with the Schrödinger equation as a closed system. The source and drain are modeled as chains of hard-core bosons with equal length  $L_S = L_D = 30$ . Initially, the source is prepared at half filling ( $N_p = 15$ ) in its ground state (the ring and drain are empty) decoupled from the ring [ $K(t = 0) = 0$ ]. For  $t > 0$  the coupling is suddenly switched on [ $K(t > 0) = J$ ]. Due to numerical limitations, we analyze the short-time dynamics. For the open system, the reservoirs obey the Pauli principle with  $r = 0.65$  and  $\Gamma = 1.5$ . (d) Solid lines: The steady-state current ( $j_{ss}$ ) we obtained applying the method presented in Refs. [39,40] for noninteracting particles with  $L = 100$ . Dashed lines: A fit ( $\epsilon = \{0.15, 0.49\}$ ) with the transmission equations derived by Büttiker *et al.* [11]. (e)  $j_{ss}$  for an infinite on-site interaction in both leads and ring plotted against flux  $\Phi$  and fractional statistics  $\eta$  ( $\eta = \{0, 2\}$  noninteracting fermions,  $\eta = 1$  hard-core bosons, else anyons) for a strong source-drain imbalance. The reservoirs obey the Pauli principle with  $r = 0$ ,  $\Gamma = 1/2$ . The number of ring sites is  $L/2 = 3$  and the ring-lead coupling is  $K/J = 1$ . At the transition to bosons, there is a discontinuity in the current. (f)–(h)  $j_{ss}$  for hard-core bosons, anyons ( $\eta = 0.25$ ), and fermions plotted against flux and the filling factor  $n_s$ . The reservoirs can have multiple particles per state and have a small particle number imbalance between the source and drain with  $n_s - n_D = 0.01$ . The current is normalized to one for each value of filling independently.

for the reduced density matrix (tracing out the baths) [41]. The bath-lead coupling is assumed to be weak and within the Born-Markov approximation. We consider two types of reservoirs: The first type allows multiple particles per reservoir state  $L_1 = \sqrt{\Gamma n_S} \hat{a}_S^\dagger$ ,  $L_2 = \sqrt{\Gamma(n_S + 1)} \hat{a}_S$ ,  $L_3 = \sqrt{\Gamma n_D} \hat{a}_D^\dagger$ , and  $L_4 = \sqrt{\Gamma(n_D + 1)} \hat{a}_D$  [ $n_S$  ( $n_D$ ) is the density of the source (drain) site if uncoupled to the ring].

The other type is restricted to a single particle per state (Pauli principle)  $L_1 = \sqrt{\Gamma}\hat{a}_S^\dagger$ ,  $L_2 = \sqrt{r}\Gamma\hat{a}_S$ , and  $L_3 = \sqrt{\Gamma}\hat{a}_D$  ( $r$  characterizes the backtunneling into the source reservoir). We solve the equations for the steady state of the density matrix  $\frac{\partial \rho_{SS}}{\partial t} = 0$  numerically [42]. The current operator is  $j = -iK(\hat{a}_S^\dagger\hat{a}_0 - \hat{a}_0^\dagger\hat{a}_S)$  and its expectation value is  $\langle j \rangle = \text{Tr}(j\rho_{SS})$ . We generalize the particle statistics with the parameter  $\eta$  ( $\eta = \{0, 2\}$  fermions,  $\eta = 1$  bosons, else anyons) using the transformation  $\hat{a}_n^\dagger \rightarrow \hat{a}_n^\dagger \prod_{j=n+1}^L e^{i\pi(1-\eta)\hat{n}_j}$  [43–45]. In Figs. 4(a)–4(c), we compare the open-system Lindblad approach with a full simulation of both ring and reservoirs using DMRG (density matrix renormalization group—see details in the caption and Supplemental Material [35]) [46,47]. Both methods yield similar results, with the Lindblad approach smoothing out the oscillation found in DMRG. This shows that leads modeled as a Markovian bath without memory are sufficient to describe the dynamics. Using both methods, we calculate the evolution towards the steady state. Remarkably, for the current, the *initial dynamics depends on the flux*, showing the Aharonov-Bohm effect of the dynamics. However, we find surprisingly that *the steady-state reached after long times is nearly independent of flux*.

For vanishing atom-atom interactions, the equilibrium scattering-based results of Büttiker *et al.* [11] and the nonequilibrium steady-state current yield a similar result [Fig. 4(d)]. Next, we enforce the Pauli principle ( $U = \infty$ ) in both leads and ring and vary the particle statistics and the average number of particles in the system (filling factor). Fermions are then noninteracting, while anyons and bosons interact more strongly with increasing filling. Now, we use the open-system method to characterize the steady-state current. We found that the type of particle and interparticle interaction has a profound influence on the Aharonov-Bohm effect [Figs. 4(e)–4(h)]. While noninteracting fermions or bosons react strongly to an applied flux, interacting bosons have only a weak dependence on the flux. Fermions have zero current at the degeneracy point, while anyons have a specific point with minimal current, which depends on the reservoir properties. When the filling of atoms in the ring is increased, fermions show no change in the current. However, for anyons a shift of the Aharonov-Bohm minimum in flux is observed. The minimum weakens the closer the statistical factor is to the bosonic exchange factor. For hard-core bosons, we find that the current becomes minimal at half flux for low filling, however, *vanishes with increasing filling*. The scattering between atoms increases with the filling factor, washing out the Aharonov-Bohm effect.

#### IV. DISCUSSION

The dynamics of atoms in the ring device can be controlled with the ring-lead coupling and flux. In general, the interaction between atoms washes out the well-defined oscillations of current between the source and drain. However, the effect of the interaction depends specifically also on the geometry. For odd parity, the interaction between the atoms does not have a significant influence on the dynamics. Using the flux, it is possible to switch the transmission through the device for even parity.

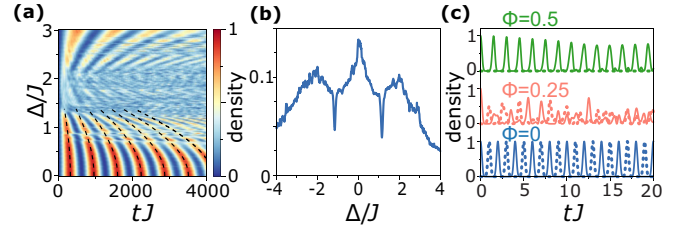


FIG. 5. Applications. (a) Density in the drain plotted against two potential barriers placed symmetrically in both arms of the ring with depth  $\Delta$ .  $L = 14$ ,  $N_p = 4$ ,  $K/J = 0.1$ , and  $U/J = 3$ . The dashed line indicates a fit with the analytic formula for the oscillation period used for the flux dependence in Figs. 3(a) and 3(b) [Supplemental Material Eq. (10), replace  $\Phi$  with  $\Delta/(2J)$ ]. (b) Average density in the drain integrated over a time  $t = 10\,000/J$  for a potential well with depth  $\Delta$  in one arm of the ring. Interference effects cause minima in the transmission rate for certain values of  $\Delta$ .  $L = 14$ ,  $N_p = 4$ ,  $K/J = 1$ , and  $U/J = 0.1$ . (c) Density in the source (solid) and drain (dashed) with the perfect state transfer protocol with  $U/J = 0$  and  $L = 14$ . Atoms oscillate between the source and drain with period  $t = 2$ .

We find that the current through this device depends strongly on the particle statistics. Fermions behave fundamentally differently from bosons. Fermions show a strong Aharonov-Bohm effect, which has been studied in mesoscopic devices. However, interacting bosons have not been realized in a mesoscopic device. *Remarkably, for interacting bosons in the strong-coupling regime, the Aharonov-Bohm effect is effectively suppressed.* Indeed, the Aharonov-Bohm effect results from a gauge field that breaks time-reversal symmetry and modifies the phase of particles traveling along the two paths of the ring. Interacting bosons can condense with the emergence of a condensate phase. Our results indicate that this condensate phase is able to cancel the phase shift induced by the Aharonov-Bohm effect and suppress it in interacting bosons. Surprisingly, we find that even in the nonequilibrium dynamics we studied the Aharonov-Bohm effect remains suppressed. Our study of the transport of anyonic particles confirms that the statistical factors can modify the interference: The anyon statistical factor is found to be able to both move the Aharonov-Bohm minimum and weaken the dependence of the interference on the applied flux.

In summary, the Aharonov-Bohm effect in the mesoscopic regime does experience a nontrivial crossover as a function of the interaction, carrier statistics, and the ring-lead coupling strength. Using cold atoms, this device would allow one to observe these effects for bosons.

Here, we present possible applications using the physics discussed above. We study them in the closed ring-lead configuration, with the atoms initially in the source. These devices could be readily realized in cold-atom experiments.

*dc-SQUID.* First, we study the atomtronic counterpart of the dc superconducting quantum interference device (dc-SQUID): We change the local potential by  $\Delta$  at two single sites in the ring symmetrically in the upper and lower half by adding the following part to the Hamiltonian:  $\mathcal{H}_{\text{imp}} = \Delta(\hat{n}_{\lceil L/4 \rceil} + \hat{n}_{\lfloor 3L/4 \rfloor})$ . The time evolution depending on  $\Delta$  is shown in Figs. 5(a) and 5(b). The potential barrier modifies the transfer rate to the drain in a quantitatively similar way

as the Aharonov-Bohm flux. However, no destructive interference is observed. This indicates that the barrier influences the dynamics only by scattering incoming particles, but does not imprint a phase shift. However, by adjusting  $\Delta$  we can control the source-drain transfer rate in a similar fashion as the flux. This device would realize an easily controllable atomtronic transistor.

*Quantum-dot simulator.* Next, we study the propagation through a quantum-dot-like structure [48,49]. Here, the local potential is changed by adding a potential well on one arm of the ring,  $\mathcal{H}_{\text{qd}} = \Delta \sum_{j=0}^{\lfloor (L-6+\text{mod}(L,4))/2 \rfloor} \hat{n}_j$ . We found that distinct transmission minima are displayed [see Fig. 5(c)]. Such results indicate that the atoms acquire a phase difference while traveling through the ring. This device could realize a switch by changing  $\Delta$  around the transmission minima, or alternatively a simulator for quantum dots.

*Perfect state transfer.* Finally, we investigate the perfect state transfer protocol, where particles move from the source to drain and vice versa without dispersion at a fixed rate [50]. The coupling parameters are  $J_n = \frac{\pi}{2} J \sqrt{s_n} \sqrt{n(L_0 - n)}$ , where  $n$  is the numeration of the coupling from the source to drain,  $L_0 = L/2 + 3$  the number of sites on the shortest path between the source and drain, and  $s_n$  secures the Kirchhoff's law. We set  $s_n = 1$  everywhere except at the two ring sites which are coupled directly to the leads: There, the coupling of those sites to the neighboring two ring sites is  $s_n = 1/2$ . The flux dependence of the time evolution of the density for  $U = 0$  is shown in Fig. 5(c). At  $\Phi = 0$  we observe that the density in the source and drain oscillates at a constant rate with close to unit probability. Depending on the interaction and particle number, the fidelity of the transport remains at unity or decreases. We will study this interesting effect in a future publication. In contrast to weak coupling, the particles move as a wave packet inside the ring. By tuning the flux, the drain density can be controlled and transmission to the drain becomes zero at the degeneracy point. The setup with the perfect state transfer could realize a switch or atomtronic quantum interference transistors: By changing the flux, perfect transmission is changed into perfect reflection. We note that our system can be relevant for a Mach-Zehnder matter-wave interferometer with enhanced flexibility and control (see Refs. [51–53]). The setup is a tool to test the quantum foundation with an interaction-free measurement. In particular, we propose to use the high control over the dynamics to create an atomic version of a Elitzur-Vaidman bomb tester, the hallmark example of an interaction-free measurement [54]. The system is prepared with a single particle, the flux set to the degeneracy point, and

a bomb, which is triggered when the particle is measured in one specific arm of the ring. Without the bomb, the Aharonov-Bohm effect prevents the particle from reaching the drain. Only if there is a bomb and the particle has not triggered it, the particle reaches the drain with unit probability due to the perfect state transfer. This setup has a 50% chance to detect the bomb without detonating it, improving from the 33% efficiency of the photonic implementation.

## V. CONCLUSION

We studied the nonequilibrium transmission through an Aharonov-Bohm mesoscopic ring. By quenching the spatial confinement, the dynamics is strongly affected by the leading coupling, the parity of the ring sites, and the interaction of the atoms. By combining our analysis with the study of the nonequilibrium steady states in an open system, we find that the Aharonov-Bohm effect is washed out for interacting bosons. Finally, we have analyzed the possible implications of our study to conceive new quantum atomtronic devices.

We believe our study will be instrumental to bridge cold-atom and mesoscopic physics and create a tool to explore new areas of research. In particular, our approach effectively defines possible directions in quantum transport: Important chapters of the field, such as full counting statistics and shot noise [55], matter-wave interferometers, rotation sensors, and non-Markovian dynamics [56] could be studied with the twist provided by the cold-atom quantum technology. Most of the physics we studied here could be explored experimentally with the current know-how in quantum technology and cold atoms. In particular, flux in ring condensates [57] or clock transitions [58], lattice rings [59], and quench dynamics in leads [60] have been demonstrated with recent light-shaping techniques [61]. Atom dynamics can be measured via fluorescence or absorption imaging of the density or current [62]. Our results can be relevant in other contexts of quantum technology, beyond ultracold atoms [63].

## ACKNOWLEDGMENTS

We thank A. Leggett for enlightening discussions. The Grenoble LANEF framework (Grant No. ANR-10-LABX-51-01) is acknowledged for its support with mutualized infrastructure. We thank National Research Foundation Singapore and the Ministry of Education Singapore Academic Research Fund Tier 2 (Grant No. MOE2015-T2-1-101) for support.

- [1] Y. Aharonov and D. Bohm, *Phys. Rev.* **115**, 485 (1959).
- [2] S. Olariu and I. I. Popescu, *Rev. Mod. Phys.* **57**, 339 (1985).
- [3] L. Vaidman, *Phys. Rev. A* **86**, 040101(R) (2012).
- [4] A. J. Leggett, *Suppl. Prog. Theor. Phys.* **69**, 80 (1980).
- [5] A. M. Lobos and A. A. Aligia, *Phys. Rev. Lett.* **100**, 016803 (2008).
- [6] J. Rincón, K. Hallberg, and A. A. Aligia, *Phys. Rev. B* **78**, 125115 (2008).

- [7] P. M. Shmakov, A. P. Dmitriev, and V. Y. Kachorovskii, *Phys. Rev. B* **87**, 235417 (2013).
- [8] O. Hod, R. Baer, and E. Rabani, *Phys. Rev. Lett.* **97**, 266803 (2006).
- [9] E. A. Jagla and C. A. Balseiro, *Phys. Rev. Lett.* **70**, 639 (1993).
- [10] Y. Gefen, Y. Imry, and M. Y. Azbel, *Phys. Rev. Lett.* **52**, 129 (1984).

- [11] M. Büttiker, Y. Imry, and M. Y. Azbel, *Phys. Rev. A* **30**, 1982 (1984).
- [12] R. A. Webb, S. Washburn, C. P. Umbach, and R. B. Laibowitz, *Phys. Rev. Lett.* **54**, 2696 (1985).
- [13] A. Nitzan and M. A. Ratner, *Science* **300**, 1384 (2003).
- [14] N. Byers and C. Yang, *Phys. Rev. Lett.* **7**, 46 (1961).
- [15] F. Bloch, *Phys. Rev.* **166**, 415 (1968).
- [16] L. Gunther and Y. Imry, *Solid State Commun.* **7**, 1391 (1969).
- [17] A. Bachtold, C. Strunk, J.-P. Salvetat, J.-M. Bonard, L. Forró, T. Nussbaumer, and C. Schönenberger, *Nature (London)* **397**, 673 (1999).
- [18] U. C. Coskun, T.-C. Wei, S. Vishveshwara, P. M. Goldbart, and A. Bezryadin, *Science* **304**, 1132 (2004).
- [19] D. M. Cardamone, C. A. Stafford, and S. Mazumdar, *Nano Lett.* **6**, 2423 (2006).
- [20] Y. Aharonov and A. Casher, *Phys. Rev. Lett.* **53**, 319 (1984).
- [21] D. J. Papoular, L. P. Pitaevskii, and S. Stringari, *Phys. Rev. Lett.* **113**, 170601 (2014).
- [22] A. Li, S. Eckel, B. Eller, K. E. Warren, C. W. Clark, and M. Edwards, *Phys. Rev. A* **94**, 023626 (2016).
- [23] S. Krinner, D. Stadler, D. Husmann, J.-P. Brantut, and T. Esslinger, *Nature (London)* **517**, 64 (2015).
- [24] D. Husmann, S. Uchino, S. Krinner, M. Lebrat, T. Giamarchi, T. Esslinger, and J.-P. Brantut, *Science* **350**, 1498 (2015).
- [25] B. T. Seaman, M. Krämer, D. Z. Anderson, and M. J. Holland, *Phys. Rev. A* **75**, 023615 (2007).
- [26] R. Dumke, Z. Lu, J. Close, N. Robins, A. Weis, M. Mukherjee, G. Birkl, C. Hufnagel, L. Amico, M. G. Boshier, K. Dieckmann, W. Li, and T. C. Killian, *J. Opt.* **18**, 093001 (2016).
- [27] L. Amico, G. Birkl, M. Boshier, and L.-C. Kwek, *New J. Phys.* **19**, 020201 (2017).
- [28] J. Dalibard, F. Gerbier, G. Juzeliūnas, and P. Öhberg, *Rev. Mod. Phys.* **83**, 1523 (2011).
- [29] C. Ryu and M. G. Boshier, *New J. Phys.* **17**, 092002 (2015).
- [30] L. Angers, F. Chiodi, G. Montambaux, M. Ferrier, S. Guéron, H. Bouchiat, and J. C. Cuevas, *Phys. Rev. B* **77**, 165408 (2008).
- [31] A. Tokuno, M. Oshikawa, and E. Demler, *Phys. Rev. Lett.* **100**, 140402 (2008).
- [32] M. Atala, M. Aidelsburger, M. Lohse, J. T. Barreiro, B. Paredes, and I. Bloch, *Nat. Phys.* **10**, 588 (2014).
- [33] M. Aidelsburger, M. Lohse, C. Schweizer, M. Atala, J. T. Barreiro, S. Nascimbène, N. Cooper, I. Bloch, and N. Goldman, *Nat. Phys.* **11**, 162 (2015).
- [34] M. Aidelsburger, *Artificial Gauge Fields with Ultracold Atoms in Optical Lattices* (Springer, Berlin, 2015).
- [35] See Supplemental Material at <http://link.aps.org/supplemental/10.1103/PhysRevA.100.041601> for the derivation of the analytic results for the dynamics in the non-interacting case and shows the cross-over from weak to strong coupling. Further results on applications for zero interaction is shown.
- [36] M. Valiente and D. Petrosyan, *J. Phys. B* **41**, 161002 (2008).
- [37] M. R. Sturm, M. Schlosser, R. Walser, and G. Birkl, *Phys. Rev. A* **95**, 063625 (2017).
- [38] L. Glazman and M. Pustilnik, in *New Directions in Mesoscopic Physics (Towards Nanoscience)*, edited by R. Fazio, V. F. Gantmakher, and Y. Imry, NATO Science Series II: Mathematics, Physics and Chemistry (Springer, Berlin, 2003), Vol. 125, pp. 93–115.
- [39] T. Prosen, *New J. Phys.* **10**, 043026 (2008).
- [40] C. Guo and D. Poletti, *Phys. Rev. A* **95**, 052107 (2017).
- [41] H.-P. Breuer and F. Petruccione, *The Theory of Open Quantum Systems* (Oxford University Press, Oxford, UK, 2002).
- [42] C. Guo and D. Poletti, *Phys. Rev. B* **96**, 165409 (2017).
- [43] L. Amico, A. Osterloh, and U. Eckern, *Phys. Rev. B* **58**, R1703 (1998).
- [44] T. Keilmann, S. Lanzmich, I. McCulloch, and M. Roncaglia, *Nat. Commun.* **2**, 361 (2011).
- [45] S. Greschner and L. Santos, *Phys. Rev. Lett.* **115**, 053002 (2015).
- [46] S. R. White and A. E. Feiguin, *Phys. Rev. Lett.* **93**, 076401 (2004).
- [47] E. M. Stoudenmire and S. R. White, ITensor Library (version 2.1.1), <http://itensor.org/>.
- [48] A. Levy Yeyati and M. Büttiker, *Phys. Rev. B* **52**, R14360 (1995).
- [49] J. Wu, B.-L. Gu, H. Chen, W. Duan, and Y. Kawazoe, *Phys. Rev. Lett.* **80**, 1952 (1998).
- [50] L. Dai, Y. Feng, and L. Kwek, *J. Phys. A: Math. Theor.* **43**, 035302 (2009).
- [51] T. Berrada, S. van Frank, R. Bücker, T. Schumm, J.-F. Schaff, and J. Schmiedmayer, *Nat. Commun.* **4**, 2077 (2013).
- [52] Y. Ji, Y. Chung, D. Sprinzak, M. Heiblum, D. Mahalu, and H. Shtrikman, *Nature (London)* **422**, 415 (2003).
- [53] C. Sturm, D. Tanese, H. Nguyen, H. Flayac, E. Galopin, A. Lemaître, I. Sagnes, D. Solnyshkov, A. Amo, G. Malpuech *et al.*, *Nat. Commun.* **5**, 3278 (2014).
- [54] A. C. Elitzur and L. Vaidman, *Found. Phys.* **23**, 987 (1993).
- [55] I. Lovas, B. Dóra, E. Demler, and G. Zaránd, *Phys. Rev. A* **95**, 053621 (2017).
- [56] A. Chiuri, C. Greganti, L. Mazzola, M. Paternostro, and P. Mataloni, *Sci. Rep.* **2**, 968 (2012).
- [57] K. C. Wright, R. B. Blakestad, C. J. Lobb, W. D. Phillips, and G. K. Campbell, *Phys. Rev. Lett.* **110**, 025302 (2013).
- [58] W. Lai, Y.-Q. Ma, L. Zhuang, and W. M. Liu, *Phys. Rev. Lett.* **122**, 223202 (2019).
- [59] L. Amico, D. Aghamalyan, F. Auksztol, H. Crepaz, R. Dumke, and L. C. Kwek, *Sci. Rep.* **4**, 4298 (2014).
- [60] S. Eckel, J. G. Lee, F. Jendrzejewski, C. J. Lobb, G. K. Campbell, and W. T. Hill III, *Phys. Rev. A* **93**, 063619 (2016).
- [61] G. Gauthier, I. Lenton, N. M. Parry, M. Baker, M. Davis, H. Rubinsztein-Dunlop, and T. Neely, *Optica* **3**, 1136 (2016).
- [62] R. Mathew, A. Kumar, S. Eckel, F. Jendrzejewski, G. K. Campbell, M. Edwards, and E. Tiesinga, *Phys. Rev. A* **92**, 033602 (2015).
- [63] P. Roushan, C. Neill, A. Megrant, Y. Chen, R. Babbush, R. Barends, B. Campbell, Z. Chen, B. Chiaro, A. Dunsworth *et al.*, *Nat. Phys.* **13**, 146 (2017).